

EBSD Based Analysis of Lead Free Solders

Extracted from an application note by T.R. Bieler, B.C. Ng, A.U. Telang and M.A. Crimp
Michigan State University, East Lansing, MI 48824

with additional work by Matt Nowell - *EDAX*

Introduction

One of the challenges of the electronic packaging industry is to move from traditional lead based solders to lead-free solders in order to reduce the use of toxic materials. However, one of the obstacles to moving to lead-free solders is cracking of the solder joints. Current characterization tools being used to solve this problem are basic SEM imaging and EDS.

EBSD offers new possibilities for characterizing cracking in solders. Often SEM imaging suggests that the cracks are intergranular – that is, they propagate at grain boundaries. However, this is not always obvious from SEM images alone. EBSD can unambiguously identify cracks as intergranular or transgranular. In addition, statistical analysis of grain boundaries can identify the types of grain boundaries that may be susceptible or resistant to cracking. EBSD is also capable of identifying areas of high local orientation variations which are indicative of the buildup of localized residual strain. If the stress state can be accurately determined then the anisotropy of elastic stiffness or incompatibility at grain boundaries can also be modeled. Such analyses done over a matrix of specimens can help identify potential process improvement opportunities.

Sample Preparation

EBSD is very much a surface sensitive technique sampling only 10 to 20nm in to the depth of the sample. Thus, in order to get good EBSD data it is imperative to have a well prepared sample surface. Lead free solders pose some particular difficulties for sample preparation for EBSD due to the softness of the solder, and the relative hardness differences between the solder alloy, the contact metal layers, and the intermetallic phases present. Often polishing times and forces will need to be reduced for optimal results. In addition, polishing to the correct plane within the sample can be difficult. A procedure recommended by Allied High Tech Products, Inc. is listed in Table 1. Providing an adequate path to ground during analysis to minimize charging effects can also be problematic. Often samples are embedded in a non-conductive epoxy to facilitate preparation. This provides a large non-conducting volume around the sample. One approach is to sputter deposit a thin (25-35Å) conductive carbon layer over the sample surface. However careful control of the film thickness is required to minimize EBSD pattern degradation. Another approach is to use a conductive paint (carbon or silver) to cover most of the sample surface area except for the region of interest. This can be accompanied by a thinner (10-15Å) carbon coat. A third

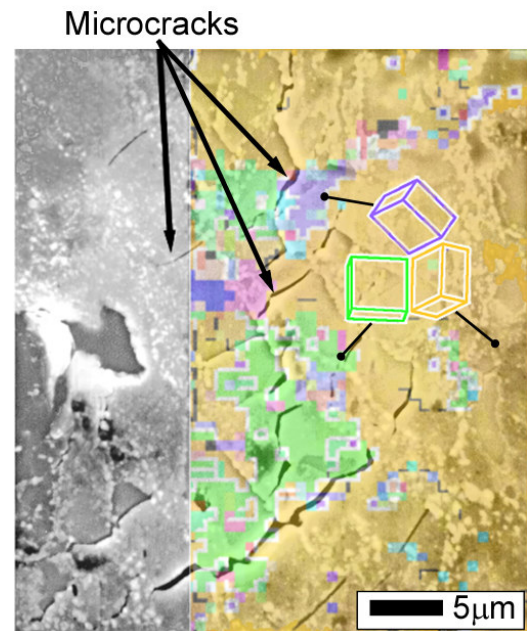


Figure 1 – Micrograph of a lead-free solder partially overlaid with an orientation map. Colored tetragons show the orientation of the colored regions in the map. (Courtesy of T. Bieler – Michigan State University)

approach is to add conductive filler to the epoxy; however this can make sectioning to the desired plane more difficult. A fourth option, if applicable, is to use the low vacuum analysis capability available on many modern SEMs.

Table 1 - Sample Preparation Procedure for Lead-Free Solders (Allied High-Tech Products, Inc.)

Step	1	2	3	4	5	6
Abrasive	320 Grit SiC Grinding Paper	600 Grit SiC Grinding Paper	6µm Polycrystalline Diamond Suspension	3µm Polycrystalline Diamond Suspension	1µm Polycrystalline Diamond Suspension	0.05µm Colloidal Silica
Polishing Cloth	NA	NA	Gold Label	White Label	Vel Cloth	ChemPol
Coolant	Water	Water	GreenLube	GreenLube	GreenLube	Water
Pressure	10 lb/F	10 lb/F	8 lb/F	8 lb/F	8 lb/F	5 lb/F
Time	2:00	2:00	6:00	3:30	3:30	2:00
Platen Speed	250 RPM Complementary	250 RPM Complementary	150 RPM Complementary	150 RPM Complementary	150 RPM Complementary	150 RPM Complementary
Polishing Head Speed	150 RPM	150 RPM	150 RPM	150 RPM	150 RPM	150 RPM

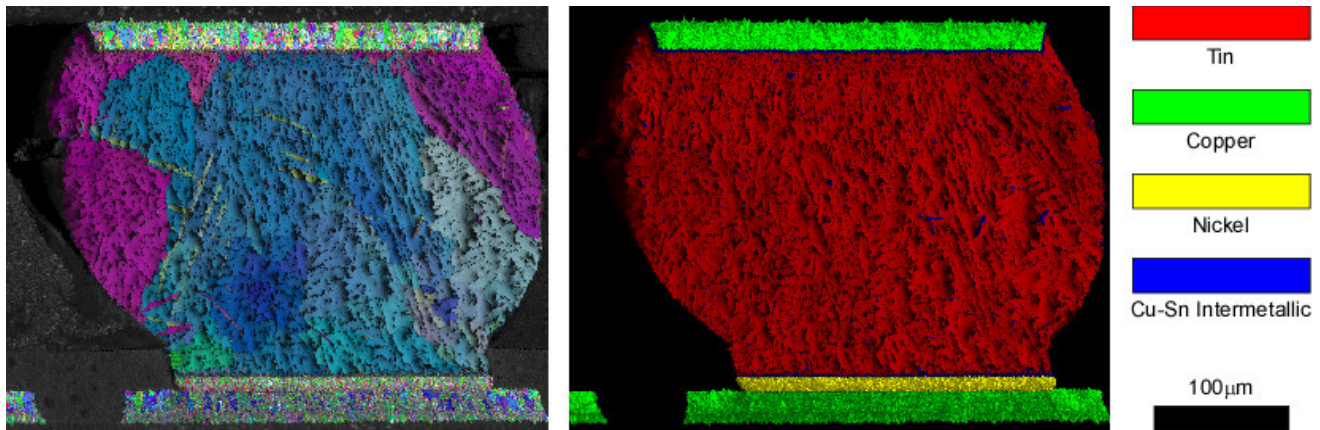


Figure 2 – Orientation map and phase map from a lead-free solder bump.

Grain Boundary Sliding in a Lead-Free Solder Joint

OIM has been used to study the mechanisms leading to cracking in lead-free solder joints. OIM easurements of local crystal orientations help illuminate the process of damage nucleation. Lead-free solders have complex slip system behavior due to their inherent tetragonal crystal structure. For example, in low strain rate creep/thermal cycling experiments on tin based solder joints (Figure 3), grain boundary sliding on low angle boundaries (shown in Figure 4) resulted in minimal crystal rotations, whereas deformation at higher rates resulted in polyslip conditions that caused significant and predictable rotations using polycrystal plasticity models.

In Sn-Ag solder, most joints are nearly single crystals, resulting from the fact that crystal nucleation is very difficult

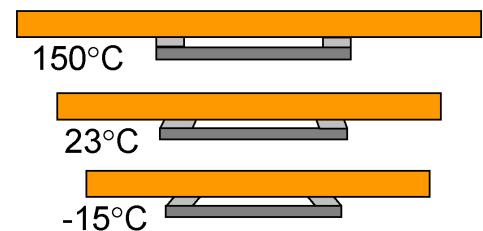


Figure 4 - Schematic diagram of thermal cycling strains due to differential expansion between a copper substrate and a nickel simulated surface mount component. 4 hr cycle, 20 min 150C, 3.5 hr -15C.

due to Sn's high enthalpy of fusion. In some systems such as the one shown schematically in figure 3, thermal cycling causes differential strains between the copper substrate and a surface mount component. In the solder joint, the differential strains have led to sliding phenomena at on low angle boundaries as illustrated in Figure 4 for the left joint. These boundaries were found to be low angle coincident site lattice boundaries. This is contrary to conventional wisdom that such boundaries would be resistant to grain boundary sliding. With thermal cycling, the initially strong single orientation was broken up into sub grains, weakening the initial texture, as evident in comparing both the discrete and density pole figures in 4(a) and 4(b). The OIM orientation data can be coupled with a finite-element model (FEM) to calculate Schmid Factors. Schmid factors give an indication of a grain's propensity to slip given the orientation of slip planes in the grain (as can be determined from the OIM data) and the local stress state (as computed by FEM). This information can be used to visualize slip systems and their relationship to grain boundary sliding. The ellipses on the right side of Figure 4(b) represent unit circles tilted on the plane indicated (the major axis is the plane trace). Slip directions with high Schmid factors are indicated. Sliding correlates closely with the highly stressed slip systems.

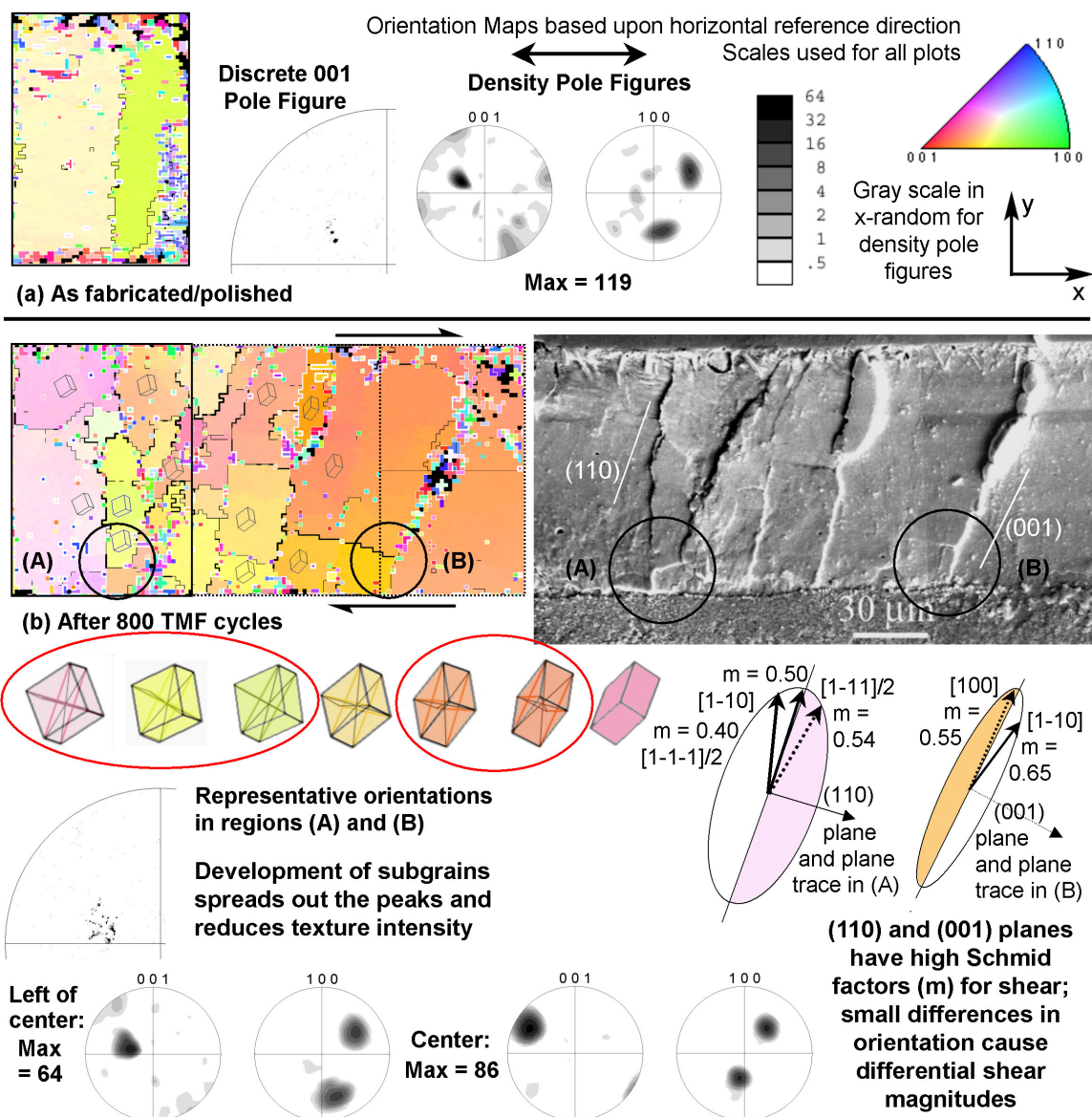


Figure 5 - Left joint of thermomechanically fatigued solder joint specimen, (a) orientation map of as-fabricated initially polished surface of specimen, (b) after 800 TMF cycles between -15 °C and 150°C.

Conclusions

With proper sample preparation, OIM can be used to characterize the mechanisms that lead to cracking in lead-free solder joints. The goal is to correlate these observations with parameteric studies to improve the cracking resistance of lead-free solder joints.

Bibliography

Scientific publications documenting the application of EBSD to Lead Free Solders

- E. Anderson (2007). "Development of Sn-Ag-Cu and Sn-Ag-Cu-X alloys for Pb-free electronic solder applications." *Journal of Materials Science: Materials in Electronics* **18**: 55-76
- P. Borgesen, T. R. Bieler, L. P. Lehman and E. J. Cotts (2007). Pb-Free Solder: New Materials Considerations for Microelectronics Processing. *MRS Bulletin*. **32**: 360-364.
- J. Gong, C. Liu, P. P. Conway and V. V. Silberschmidt (2007). "Micromechanical modelling of SnAgCu solder joint under cyclic loading: Effect of grain orientation." *Computational Materials Science* **39**: 187-197
- D. W. Henderson, M. A. Korhonen, T.-M. K. Korhonen and L. P. Lehman (2007). "Isothermal fatigue behavior of the near-eutectic Sn-Ag-Cu alloy between -25°C and 125°C." *Journal of Electronic Materials* **36**: 173-178
- P. P. Jud, G. Grossmann, U. Sennhauser and P. J. Uggowitzer (2006). "Local fatigue in lead-free SnAg3.8Cu0.7 solder." *Advanced Engineering Materials* **8**: 179-183
- T.-M. K. Korhonen, P. Turpeinen, L. P. Lehman, B. Bowman, G. H. Thiel, R. C. Parkes, M. A. Korhonen, D. W. Henderson and K. J. Puttlitz (2004). "Mechanical properties of near-eutectic Sn-Ag-Cu alloy over a wide range of temperatures and strain rates." *Journal of Electronic Materials* **33**: 1581-1588
- V. Kumar, Z. Z. Fang, J. Liang and N. Dariavach (2006). "Microstructural Analysis of Lead-Free Solder Alloys." *Metallurgical and Materials Transactions A* **37A**: 2505-2514
- Lalonde, D. Emelander, I. J. Jeannette, C. Larson, W. Rietz, D. Swenson and D. W. Henderson (2004). "Quantitative metallography of p-sn dendrites in Sn-3.8ag-0.7Cu ball grid array solder balls via electron backscatter diffraction and polarized light microscopy." *Journal of Electronic Materials* **33**: 1545-1549
- J. G. Lee, A. U. Telang, K. N. Subramanian and T. R. Bieler (2002). "Modeling Thermomechanical Fatigue Behavior of Sn-Ag Solder Joints." *Journal of Electronic Materials* **31**: 1152-1159
- D. Li, C. Liu and P. P. Conway (2005). "Characteristics of intermetallics and micromechanical properties during thermal ageing of Sn-Ag-Cu flip-chip solder interconnects." *Materials Science and Engineering A* **391**: 95-103
- M. A. Matin, W. P. Vellinga and M. G. D. Geers (2006). "Microstructure evolution in a Pb-free solder alloy during mechanical fatigue." *Materials Science and Engineering A* **431**: 166-174
- M. A. Matin, W. P. Vellinga and M. G. D. Geers (2007). "Thermomechanical fatigue damage evolution in SAC solder joints." *Materials Science and Engineering A* **445-446**: 73-85
- J. M. Song, C. F. Huang and H. Y. Chuang (2006). "Microstructural characteristics and vibration fracture properties of Sn-Ag-Cu-TM (TM = Co, Ni, and Zn) alloys." *Journal of Electronic Materials* **35**: 2154-2163
- Swenson (2007). "The effects of suppressed beta tin nucleation on the microstructural evolution of lead-free solder joints." *Journal of Materials Science: Materials in Electronics* **18**: 39-54
- U. Telang and T. R. Bieler (2005). "The Orientation Imaging Microscopy of Lead-Free Sn-Ag Solder Joints." *JOM* **57**: 44-49
- U. Telang and T. R. Bieler (2005). "Characterization of microstructure and crystal orientation of the tin phase in single shear lap Sn-3.5Ag solder joint specimens." *Scripta Materialia* **52**: 1027-1031
- U. Telang, T. R. Bieler, S.-H. Choi and K. N. Subramanian (2002). "Orientation imaging studies of Sn-based electronic solder joints." *Journal of Materials Research* **17**: 2294-2306
- U. Telang, T. R. Bieler and M. A. Crimp (2006). "Grain boundary sliding on near-7°, 14°, and 22° special boundaries during thermomechanical cycling in surface-mount lead-free solder joint specimens." *Materials Science and Engineering A* **421**: 22-34
- U. Telang, T. R. Bieler, J. P. Lucas, K. N. Subramanian, L. R. Lehman, Y. Xing and E. J. Cotts (2004). "Grain-boundary character and grain growth in bulk tin and bulk lead-free solder alloys." *Journal of Electronic Materials* **33**: 1412-1423
- U. Telang, T. R. Bieler, D. E. Mason and K. N. Subramanian (2003). "Comparisons of Experimental and Computed Crystal Rotations Caused by Slip in Crept and Thermomechanically Fatigued Dual-Shear Eutectic Sn-Ag Solder

Joints." *Journal of Electronic Materials* **32**: 1455-1462

- U. Telang, T. R. Bieler, A. Zamiri and F. Pourboghrat (2007). "Incremental recrystallization/grain growth driven by elastic strain energy release in a thermomechanically fatigued lead-free solder joint." *Acta Materialia* **55**: 2265-2277

EDAX[®]

AMETEK[®]
MATERIALS ANALYSIS DIVISION

www.edax.com